Proton elastic and inelastic scattering at 0.8 GeV from ^{12,13}C and ^{208}Pb†

G. S. Blanpied,‡ W. R. Coker, and R. P. Liljestrand
University of Texas, Austin, Texas 78712

G. W. Hoffmann
University of Texas, Austin, Texas 78712
and Los Alamos Scientific Laboratory, Los Alamos, New Mexico 87545

L. Ray, D. Madland, C. L. Morris, J. C. Pratt, J. E. Spencer, and H. A. Thiessen
Los Alamos Scientific Laboratory, Los Alamos, New Mexico 87545

T. Kozlowski§
Brookhaven National Laboratory, Upton, New York 11973

N. M. Hintz, G. S. Kyle, and M. A. Oothoudt§
University of Minnesota, Minneapolis, Minnesota 55455

T. S. Bauer, G. Igo, R. J. Ridge,¶ and C. A. Whitten, Jr.
University of California, Los Angeles, California 90024

P. M. Lang,§ H. Nann, and K. K. Seth
Northwestern University, Evanston, Illinois 60201
(Received 9 May 1978)

Angular distributions for the elastic and inelastic scattering of 0.8 GeV protons from ^{12}C, ^{13}C, and ^{208}Pb have been measured. Reported are data for the ground, 4.4 MeV 2^+, 7.6 MeV 0^+, 9.6 MeV 3^-, and 14.1 MeV 4^+ states of ^{12}C; the ground, 3.1 MeV $1/2^+$, 3.7 MeV $3/2^-$, 6.9 MeV $5/2^+$, 7.6 MeV $5/2^-$, and 11.9 MeV (?) states of ^{13}C; and the ground, 2.6 MeV 3^-, and 3.2 MeV 5^- states of ^{208}Pb. Analyses of the elastic angular distributions are made using the partial wave formalism and the Kerman-McManus-Thaler approach to the nucleon-nucleus optical potential; a realistic spin-orbit term is included. The inelastic transitions are analyzed within the framework of the distorted-wave Born-approximation, using transition strengths consistent with previous low-energy studies of inelastic scattering. A simple single-particle-plus-excited-core model is used for ^{13}C. In terms of this analysis, an assignment of $J^\pi = (5/2,7/2)^+$ is made for the 11.9 MeV state in ^{13}C.

[NUCLEAR REACTIONS ^{12,13}C, ^{208}Pb(p,p'), $E=0.8$ GeV; measured $\sigma(\theta)$; enriched targets; resolution ≥ 80 keV, $\theta_{c.m.}=2$–$40°$, $\Delta\theta=0.2°$. Optical potential analysis, DWBA, inelastic deformation lengths, $\beta_l R$.]

I. INTRODUCTION

Recently, a number of medium energy (incident energy ~ 1 GeV) proton elastic and inelastic angular distributions, particularly on targets ^{12}C and ^{208}Pb[1-6], have stimulated new interest in what can be learned about nuclei from medium energy scattering of hadrons. Several analyses of the ^{12}C and ^{208}Pb elastic and inelastic data have been reported.[7-19].

Analyses of the elastic data can be made to focus on the information such data can provide about the neutron matter density distribution of the target nucleus. (A good review of the many techniques involving the hadron-nucleus interaction which are currently used to investigate nuclear densities is given by Rebel.[20]) The deduced neutron distributions can then be compared with predictions of various self-consistent field models of the nucleus.[21,22] When the data extend to high enough momentum transfer, 4 fm^{-1}, or more, they have been shown to be sensitive to rather fine details of the nuclear densities.[6] The analyses have been complicated by strong absorption,[23] by uncertainties in the spin-dependence of the nucleon-nucleon interaction,[6,24] and by small but subtle effects of nucleon-nucleon correlations, particularly the Pauli correlation.[18] In the case where the nucleus is nonspherical, analyses of elastic scattering alone can only give information on the monopole, or spherical, part of the density.

Only a few inelastic angular distributions at medium energies have been reported.[2,5] Within the framework of the distorted-wave Born-approx-

imation (DWBA), the transition strengths needed to fit these data involve nuclear matrix elements which have been shown to agree well with those obtained empirically in analyses of proton inelastic scattering at 10 to 100 MeV incident energies.[14, 15] However, the available inelastic data are insufficient to explore the inelastic reaction mechanism in the medium energy region, and what can be learned from inelastic scattering at medium energies is still an unanswered question. Also, for a deformed nucleus such as ^{12}C, high quality elastic *and* inelastic data are required to provide a complete picture of the target nucleus.

The first experiment to be carried out with the high resolution spectrometer (HRS) at the Clinton P. Anderson Meson Physics Facility (LAMPF) of the Los Alamos Scientific Laboratory was the study of proton elastic and inelastic scattering on $^{12, 13}$C and ^{208}Pb at 0.8 GeV incident laboratory proton energy; the data resulting from this experiment are the subject of the present work. The ^{208}Pb differential cross section data extend to a momentum transfer of 3.9 fm^{-1}, while the data for the carbon isotopes reach 4.5 fm^{-1}.

The data include inelastic angular distributions for the 3$^-$, 2.62 MeV state in ^{208}Pb as well as the 2$^+$, 4.4 MeV, 0$^+$, 7.6 MeV, and 3$^-$, 9.6 MeV states in ^{12}C; angular distributions for these same transitions at 1 GeV incident proton energy have been previously reported.[5] For the first time, we also obtain angular distributions for the 5$^-$, 3.2 MeV state in ^{208}Pb, the 4$^+$, 14.1 MeV state in ^{12}C, and for the $\frac{1}{2}^-$ ground state; $\frac{1}{2}^+$, 3.1 MeV, $\frac{3}{2}^-$, 3.7 MeV, $\frac{5}{2}^+$, 6.9 MeV, $\frac{5}{2}^-$, 7.6 MeV, and the ?, 11.9 MeV states in ^{13}C. A presentation and preliminary theoretical analysis of these data are the main purposes of the present paper. A complete tabulation of the numerical data is on deposit in PAPS.[25]

II. EXPERIMENTAL METHOD

Details of the experimental system have been reported elsewhere.[6] For this particular experiment, the targets consisted of a self-supporting ^{208}Pb foil 10.4 mg/cm^2 thick, enriched to 99.1%, a carbon target 156 mg/cm^2 thick, consisting of ^{13}C (83% by mass), ^{12}C (15%) and ^{1}H (2%), and a CH target ("Pilot B" scintillator) of thickness 86 mg/cm^2. The CH target was also used for cross section normalization as discussed below.

Since this was the initial experiment done with the HRS facility, resolution was not optimized for all targets, and a single dispersion-matched solution[26] was used for all data obtained during the experiment. A resolution of 80–120 keV for ^{208}Pb was, however, routinely obtained for angles < 23°. Windows, added to the system, increased

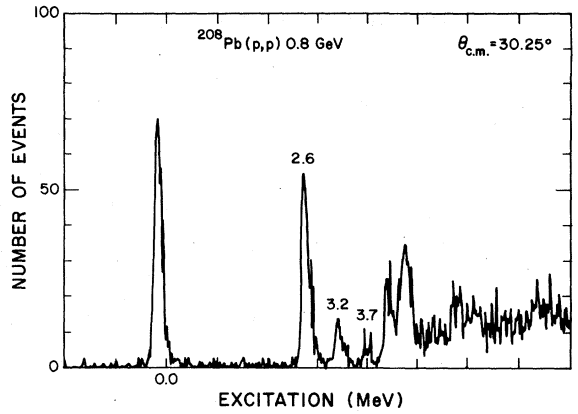

FIG. 1. The spectrum from the ^{208}Pb(p,p) reaction obtained at a laboratory scattering angle of 30°.

the resolution somewhat for data taken at laboratory angles > 23°. Figure 1 displays a ^{208}Pb(p,p) spectrum at a laboratory angle of 30°. Because the dispersion mismatch increases for larger scattering angles, and the angular uncertainty contributes to the energy resolution as $dE/d\theta$ increases, the energy resolution for light targets is worse. Thus, for the carbon isotopes the resolution was about 200 keV at the forward angles and somewhat larger at the back angles. Examples of ^{12}C and ^{13}C spectra are shown in Figs. 2 and 3,

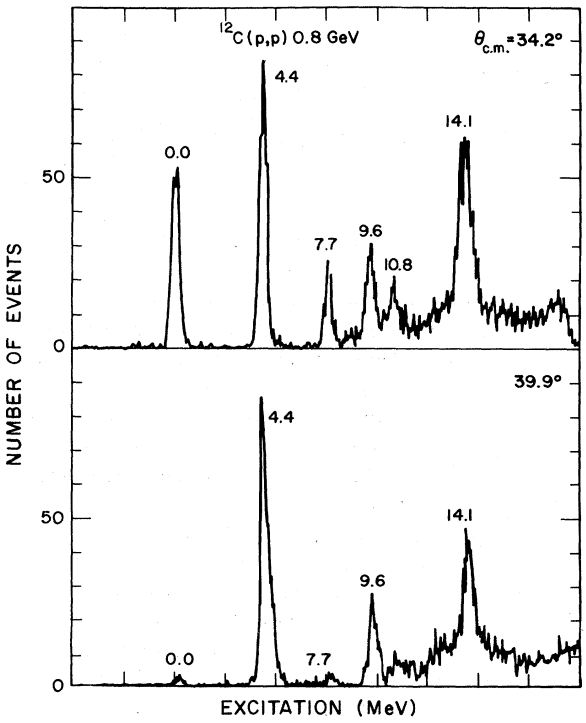

FIG. 2. Spectra from the ^{12}C(p,p) reaction at 34.2° and 39.9°.

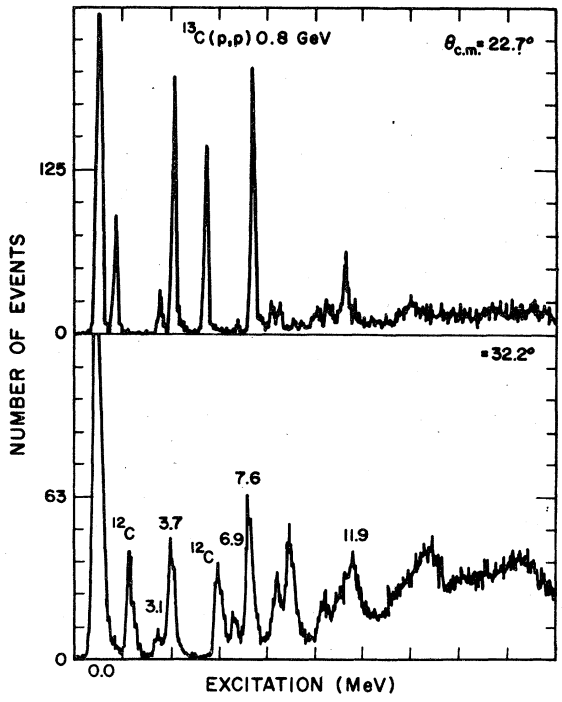

FIG. 3. Spectra from the $^{13}C(p,p)$ reaction at 22.7° and 32.2°.

respectively.

At medium incident energies, an accurate angle calibration is of extreme importance, since many nuclear structure effects which one desires to investigate show up as small angle shifts in the angular distributions. Data were obtained at 12° on either side of the incident beam and compared to determine an angle calibration that is believed to be accurate to ± 0.05°.[6] The overall normalization of the cross section data was established by taking (p,p) cross sections on the CH target and normalizing to the $^1H(p,p)$ data of Willard *et al.*[27] and of Abe *et al.*[28] The resulting nucleon-nucleus elastic scattering cross sections are accurate to ± 10%. Since the relative solid angle of the HRS varies as a function of position on the focal plane, the inelastic data were carefully normalized to the elastic data through the use of an empirically determined correction factor, which was obtained by "scanning" an elastic peak across the focal plane. Considering uncertainties in the elastic normalization, the focal plane efficiency, and background subtraction, the absolute normalization for the inelastic data is ± 12–15%, except for the 14.1 MeV state in ^{12}C and the 11.9 MeV state in ^{13}C for which it is ± 15–20%, due to a larger background subtraction.

III. THEORY

A. Elastic scattering analysis

The elastic scattering of protons from the nuclei ^{12,13}C and ^{208}Pb has been analyzed in terms of the partial-wave approach, using an optical potential generated by the method of Kerman, McManus, and Thaler[29] as modified by Feshbach *et al.*[30] In this approach, the optical potential is expanded in terms of the nuclear density. By keeping only the term to first order in the density, one takes into account nucleon-nucleon and nucleon-nucleus scattering to all orders in the scattering amplitudes, but neglects the effects of target-nucleon correlations. The only such correlations now believed to be important at medium energies are those due to the Pauli principle, and a comparison of calculations omitting and retaining these correlations shows that their omission does not affect the conclusions of the present analysis.[18,31]

The first-order term in the optical potential is sometimes called the Rayleigh-Lax (RL) potential, and is obtained in terms of the free proton-proton and proton-neutron scattering amplitudes, and the proton and neutron matter densities of the target nucleus.[32] A spin-dependent term is included in the scattering amplitudes, and gives rise to a spin-orbit term in the RL potential $U_{jl}(r)$. The Schrödinger equation is solved with exact relativistic kinematics

$$[d^2/dr^2 - l(l+1)/r^2 - 2\mu U_{jl}(r)/\hbar^2 + k_N^2]\chi_{jl}(r) = 0, \tag{1}$$

where k_N is the relativistic wave number in the proton-nucleus center-of-momentum (c.m.) system, and $\mu = \epsilon_1\epsilon_2/(\epsilon_1+\epsilon_2)$ is the "reduced energy," where ϵ_i is the total energy of particle i (proton or target nucleus) in atomic mass units, in the proton-nucleus c.m. system.[14]

The proton-nucleon scattering amplitudes used in the RL potential are taken to be of the form

$$t_{pj}(q^2) = t^0_{pj}(q^2) + it^s_{pj}(q^2)(\vec{\sigma}_p + \vec{\sigma}_j)\cdot\hat{n}, \tag{2}$$

where j stands for p or n, $\vec{q} = \vec{k}_i - \vec{k}_f$ is the momentum transfer, and $\hat{n} \equiv (\vec{k}_i \times \vec{k}_f)/|\vec{k}_i \times \vec{k}_f|$. The conventional parametrization used here is,[6] with M the nucleon mass,

$$\begin{aligned} t^0_{pj}(q^2) &= (ik_0\sigma^T_{pj}/4\pi)(1 - i\alpha_{pj})\exp(-B_{pj}q^2), \\ t^s_{pj}(q^2) &= (ik_0\theta_{pj}/4\pi)(q^2/4M^2)^{1/2} \\ &\quad \times(1 - i\alpha_{spj})\exp(-B_{spj}q^2). \end{aligned} \tag{3}$$

Nucleon-nucleon total cross section,[33–35] and very forward angular distribution data[33,36] at 0.8 GeV are used to determine $\sigma^T_{pp} = 4.73 \pm 0.05$, $\sigma^T_{pn} = 3.8$

± 0.1 fm^2, and $\alpha_{pp} = 0.06 \pm 0.08$. Dispersion theory estimates yield $\alpha_{pn} = -0.3 \pm 0.15$.[37,38] The value of α_{pj} affects only the predicted peak-to-valley ratio in the diffractive pattern of the angular distributions. Thus, α_{pn} was fixed to a value giving optimum results for a dozen target nuclei, from $A = 12$ to 208, studied at 0.8 GeV, namely $\alpha_{pn} = -0.2$. Values of $B_{pp} = 0.09 \pm 0.005$, $B_{pn} = 0.12 \pm 0.008$ fm^2 reproduce recent $p+p$ and $p+n$ angular distributions.[27,33,34,39]

Ideally the spin-dependent parameters for Eq. (3) should be obtained from complete measurements[40] of the two-nucleon system. However, this is not possible since spin correlation, double polarization, triple scattering, and other complicated measurements have not been performed near 0.8 GeV. Thus, isospin averaged spin-dependent parameters $\bar{\theta}_p$, $\bar{\alpha}_{sp}$, and $\bar{B}_{sp}$ are defined. $\bar{B}_{sp}$ is fixed at 0.2 fm^2 from preliminary $p+p$ polarization data.[41] Fitting of the polarization data allows one to determine the quantity $\theta_{pp}(\alpha_{s,pp} - \alpha_{pp})$ only and not θ_{pp} or $\alpha_{s,pp}$ separately. Thus $\bar{\theta}_p$ and $\bar{\alpha}_{sp}$ have been varied to optimize the fit to proton-*nucleus* analyzing power data on ^{12}C and ^{208}Pb as discussed in Ref. 42. The values used for the calculations reported here are (^{12,13}C) $\bar{\theta}_p = 17.6$ fm^2, $\bar{\alpha}_{sp} = 0.29$, and $\bar{B}_{sp} = 0.07$ fm^2; (^{208}Pb) $\bar{\theta}_p = 9.0$ fm^2, $\bar{\alpha}_{sp} = 0.63$, and $\bar{B}_{sp} = 0.20$ fm^2. The value of $\bar{B}_{sp} = 0.07$ fm^2 that is used for the carbon isotopes was required to obtain the fit to ^{12}C analyzing power data, shown in Fig. 2 of Ref. 42. Presumably this additional flexibility is required partially in order to simulate effects due to the large deformation of ^{12}C. Notice that although $\bar{\alpha}_{sp}$ and $\bar{\theta}_p$ have been allowed to vary from the values used for ^{208}Pb, their product is approximately constant.

Limited ^{13}C analyzing power data from about 19° to 26° laboratory angle were found to be essentially the same as the ^{12}C data, so that the same spin parameters were used for both of the carbon isotopes. In the RL potential, the nucleon-nucleon amplitudes [Eq. (2)] are summed over target-nucleon spin and convoluted with the nuclear density. For the ^{13}C system, unlike the other (0^+) nuclei considered here, the spin of the target nucleon will not vanish when summed over the nucleus, but will equal to that of the unpaired, $p_{1/2}$ neutron. This applies to the spin-dependent term included in Eq. (2) as well as other spin-dependent terms which are omitted; however, such nuclear-spin-dependent terms in the RL potential for ^{13}C carry a weight only $\frac{1}{13}$, or 8%, of the other included terms. Since the existing uncertainty in $\bar{\theta}_p \bar{\alpha}_{sp}$ is $\pm 10\%$ at present, one has little choice, for now, except to neglect the additional nuclear-spin dependent terms for ^{13}C.

A general form for the proton and neutron point density distributions was chosen as

$$\rho_j(r) = \rho_{0j}\{(1+w_j r^2/R_j^2)/[1+\exp((r^k - R_j^k)/z_j^k)] + s_j \cos(m_j r - \phi_j)\exp(-d_j(r-r_{0j})^2) + s_j' \exp(-d_j'(r-r_{0j}')^2)\}, \quad (4)$$

for $j = p$ or n and $k = 1$ for the three parameter Fermi (3pF) while $k = 2$ for the three parameter Gaussian (3pG) term. The charge form factor of the proton was numerically unfolded from the nuclear charge density, as determined from electron scattering, to yield the point-proton nuclear density parameters used in Eq. (4). The charge form factor of the proton that is used in the unfolding procedure agrees with experimental $e^- + p$ scattering data to momentum transfers of 3.3 fm^{-1},[43] while the neutron charge form factor has been neglected here. As usual, ρ_{0j} is obtained by normalizing to the proper number of target nucleons. The electron scattering data extend to about 3.5 fm^{-1} for ^{13}C, 4.0 fm^{-1} for ^{12}C, and 3.7 fm^{-1} for ^{208}Pb.[44-47] Both correction terms in Eq. (4) are needed to reproduce the high-q electron scattering data for ^{208}Pb, while the first and third terms are needed for the ^{12,13}C electron scattering data. The significance of these terms is discussed later.

Because of the large shape deformation of ^{12}C and ^{13}C, one should use a nonspherical density and replace Eq. (1) by the appropriate set of coupled equations for the ground state and such inelastic states of ^{12}C or ^{13}C as are strongly populated at 0.8 GeV incident proton energy. While we have in fact carried out such analyses of selected elastic and inelastic proton scattering data for ^{12}C, as is reported elsewhere,[48] the amount of the present data, and the aim of the present analysis to provide a survey of the kinds of nuclear structure information which can be obtained from this sort of data, are best served by a less cumbersome preliminary approach. Hence, spherical densities are used throughout, as well as the uncoupled Schrödinger equation and the distorted-wave Born-approximation.

The use of Eq. (4) is as follows. The proton densities, determined from elastic electron scattering, are kept fixed during the analysis. The neutron density parameters are varied in order to optimize simultaneously the fits to the elastic angular distributions and to the analyzing power data.[42] In this way, clearly, the effect due to nuclear deformation or due to second-order corrections (correlations) tend to be absorbed into the deduced neutron densities; we therefore refer to these densities as Rayleigh-Lax (RL) neutron densities, as distinct from the "true" neutron densities. Since calculations including deformation and Pauli correlations have been done,[18,31] the uncertainties which omission of such effects

TABLE I. The results of the theoretical analysis discussed in the text. The first four columns give the numerical values of Eq. 4. The root-mean-square (rms) radii for the point-nucleon density distributions are listed under $\langle r^2\rangle^{1/2}$. The quantity $\langle r^2\rangle_{ch}^{1/2}$ is the rms radius of the charge form factor taken from electron scattering. The errors in the neutron rms radii are ±0.10 fm for the carbon isotopes and ±0.07 fm for ^{208}Pb (Ref. 49).

Nucleus		w	R (fm)	z (fm)	k	$\langle r^2\rangle^{1/2}$ (fm)	$\langle r^2\rangle_{ch}^{1/2}$ (fm)
^{12}C	p	−0.15	2.42	0.45	1	2.319	2.453
	n	−0.15	2.43	0.46	1	2.393	
^{13}C	p	−0.16	2.51	0.41	1	2.299	2.434
	n	−0.05	2.30	0.50	1	2.54	
^{208}Pb	p	0.36	6.45	2.65	2	5.443	5.502
	n	0.36	6.19	3.13	2	5.625	

produce in $\rho_n(r)$ and in the root-mean-square neutron matter radius $\langle r_n^2\rangle^{1/2}$ are either known or can be estimated; these uncertainties are included in the statement of the results of the present analysis, (see Table I).[49]

B. Inelastic scattering

Our analysis of the inelastic scattering data for 0.8 GeV protons on targets of ^{12,13}C and ^{208}Pb was based on the distorted-wave Born-approximation (DWBA) as discussed by Satchler.[50] In this approach, well known from low-energy nuclear physics, the main ingredients are the distorted waves $\chi_{jl}(r)$ obtained by solution of Eq. (1), and a so-called "inelastic form factor," or inelastic transition density. Some previous analyses[11] of earlier medium energy inelastic scattering data have used the semiclassical Glauber approximation[51] and the Tassie model for collective nuclear excitations.[52] In the Tassie approach, one directly expands the nonspherical nuclear density in terms of Legendre polynomials.

This may be contrasted with the present approach,[14,15] which agrees with the previous conventions of low-energy nuclear physics in expanding the nuclear radius parameter $R(\hat{r})$ in Legendre polynomials. When the Raleigh-Lax potential is used, either the Tassie approach or this more conventional approach lead to the *same* result for the inelastic form factor, namely (for $S=0$ transitions),

$$F_l(r) = (\beta_l R_0)(2l+1)^{-1/2} d/dr\,[U^{RL}(r)]\ , \qquad (5)$$

where $U^{RL}(r)$ is the spin-independent part of $U_{jl}(r)$ and it was assumed only for simplicity in writing Eq. (5) that both real and imaginary parts of $U_{jl}(r)$ have the same mean radius R_0. The advantage of Eq. (5) is that values of the deformation length $\beta_l R_0$ which give the correct strength for a given inelastic transition are known from DWBA analyses of low-energy nucleon-nucleus inelastic scattering data. In the actual calculations, the (very small) effect of Coulomb excitation was also included. Inclusion of the deformed spin-orbit contribution to the inelastic form factor greatly complicates the DWBA analysis, and little is known from low-energy analyses about its strength and its importance, if any, in fitting angular distribution data. As a result, in the calculations reported here, no spin-orbit contributions were included in the inelastic form factor. This will be the subject of a future publication.[53]

We used, for the present calculations, a version of the DWBA program VENUS modified to include exact relativistic kinematics,[54] and to read in the microscopic RL potential. The number of partial waves needed varied from 40 for the carbon isotopes to 85 for ^{208}Pb. The values used, or obtained for the various theoretical parameters and the results of the calculations are discussed in the following section.

IV. RESULTS

A. ^{208}Pb

Unfolding the "model independent" charge density of Frois *et al.*[47] results in the parameters for the proton density given in Table I, plus the following values for the correction terms in Eq. (4): $s_p = -0.03$, $d_p = 0.52$ fm^{-2}, $r_{0p} = 6.3$ fm, $m_p = 1.4$ fm^{-1}, $\phi_p = 2.5$ rad, $s'_p = 0.13$, $d'_p = 0.21$ fm^{-2}, and $r'_{0p} = 0.0$ fm. Simultaneous fitting of the elastic angular distribution and analyzing power data (see Fig. 2 of Ref. 42) results in the theoretical angular distribution shown in Fig. 4 as well as the RL neutron density given in Table I. The value of the RL neutron mean square radius determined here is consistent with other analyses[11,15,55] of ~ 1 GeV elastic scattering data and with Hartree-Fock predictions.[21,22] Results obtained for this difference arising from a variety of other analyses of different types of data are given by Rebel.[20] Arguments are also given[20] which favor the analysis of the medium energy nucleon scattering data as the best technique for determining the neutron-proton rms radius difference.

An investigation[49] of the effect of systematic sources of error and model dependence on the deduced neutron rms radius has been made. Systematic errors considered were the overall normalization and determination of scattering angle of the data, beam energy, proton charge density, the two-nucleon amplitudes, and the omission in

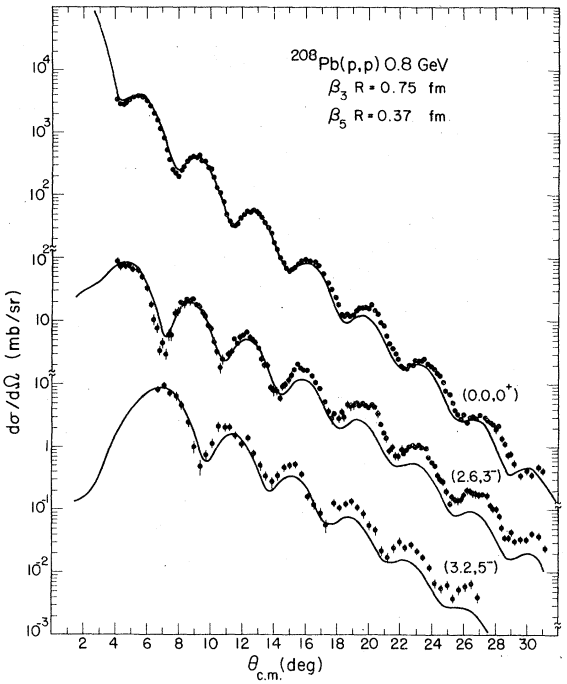

FIG. 4. Angular distributions for the ^{208}Pb ground state and excited states at 2.6 and 3.2 MeV are given, together with theoretical fits as discussed in the text.

the analysis of Pauli correlations. The procedure adopted to determine the effects on the deduced neutron densities due to all but the Pauli correlations was to individually alter each parameter and recover the original fit by variation of the neutron density. The error in the rms neutron radius due to the omission of target nucleon-nucleon correlations was estimated from the calculated changes in the overall magnitude and slope of the predicted cross sections, as given by Harrington and Varma[18] and by Boridy and Feshbach.[18] The error in the deduced neutron rms radius due to model dependence (resulting from the finite maximum momentum transfer of the data) and the statistical error in the angular distribution data was determined by generating error envelopes using approximately model-independent neutron densities. Details of the approach used here will be reported elsewhere.[49] The result of this investigation for ^{208}Pb is that the rms neutron radius is determined to ±0.07 fm. For ^{12}C, discussed below, the deduced neutron radius is determined to ±0.1 fm.

The RL potential and the distorted waves that were obtained in the analysis of elastic scattering were then used to perform DWBA calculations for the inelastic transitions to (3$^-$, 2.6 MeV) and (5$^-$, 3.2 MeV) states of ^{208}Pb, yielding the curves shown in Fig. 4. The deformation lengths are $|\beta_3 R| = 0.75$ fm and $|\beta_5 R| = 0.37$ fm, which compare very favorably with those found in low energy analyses,[56-58] which obtain on the average, values of $|\beta_3 R| = 0.79$ fm and $|\beta_5 R| = 0.36$ fm. In Ref. 58 it is noted that an energy dependence of β_5 is found when one compares the results of analyses from 25 to 61 MeV. However, since the present value of $|\beta_5 R|$ agrees with the average of the low-energy results to within 3%, it is likely that the low-energy problem was simply a consequence of optical potential ambiguities or experimental difficulties.

There is a noticeable discrepancy between the predicted slope of the inelastic angular distributions and that of the data. It has been suggested that the inclusion of the spin-orbit potential's contribution to the inelastic form factor [Eq. (5)] should remedy this discrepancy. Preliminary calculations have confirmed this conclusion; details of the analysis will appear elsewhere.[53]

B. ^{12}C and ^{13}C

For the present analysis of the ^{12,13}C elastic and inelastic scattering data, we ignore effects of channel-coupling and optical potential deformation. Elsewhere,[48] we show that such effects are vital in obtaining a resonable theoretical description of the angular distribution at 0.8 GeV for the 4$^+$, 14.1 MeV state in ^{12}C, but are of only secondary importance in the description of the elastic scattering, and the inelastic scattering to the 2$^+$, 4.4 MeV state.

The values of the 3pF form for the point proton densities [Eq. (4)] for ^{12,13}C are given in Table I. Additional Gaussian correction terms are required to reproduce electron scattering results,[45,46] and are given for ^{12}C(^{13}C) as follows: $s'_p = 0.27$ (0.33), $d'_p = 6.9$ (6.9) fm^{-2}, and $r'_{0p} = 1.4$ (1.4) fm. Notice that the difference in the rms proton radii for ^{12}C and ^{13}C as given in Table I is 0.02 fm.

Assuming $\rho_n(r) = \rho_p(r)$ for ^{12,13}C yields very poor results for the predicted versus measured elastic angular distributions beyond 25° in the c.m. system. Varying the neutron parameters to obtain good fits to the ^{12,13}C elastic cross sections yields the fits shown in Fig. 5, with neutron densities given in Table I. An additional oscillatory correction for ^{12}C was required to fit the angular distribution data beyond about 25°, the values of which are $s_n = -0.02$, $d_n = 0.33$ fm^{-2}, $r_{0n} = 2.6$ fm, $m_n = 2.7$ fm^{-1}, and $\phi_n = 1.7$ rad. For ^{13}C a Gaussian correction was used and is given by $s'_n = -0.27$, $d'_n = 4.9$ fm^{-2}, and $r'_{0n} = 1.0$ fm. One should be cautioned not to interpret these small correction terms as representing a perturbation to the actual ^{12,13}C neutron densities. Deformation effects, as well as correlations, are unaccounted for here, and

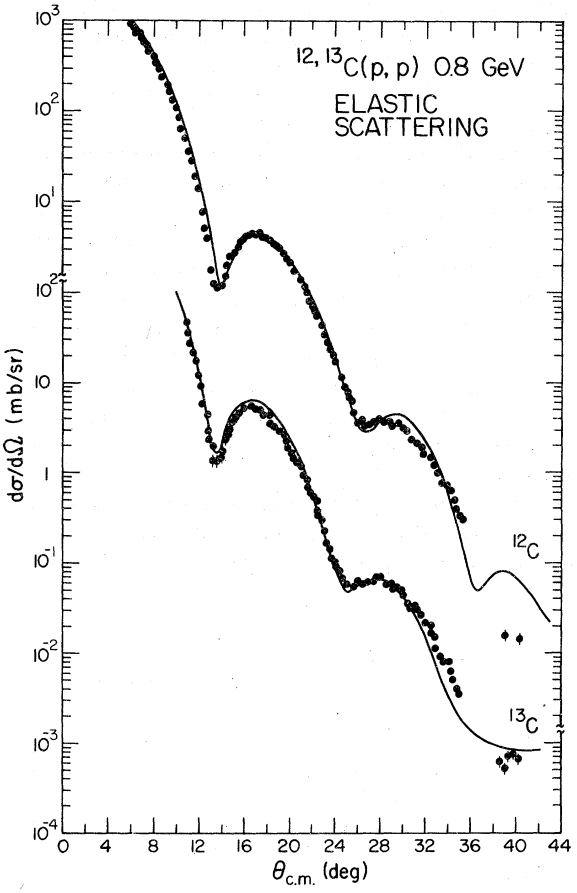

FIG. 5. Angular distributions for proton elastic scattering from ^{12}C and ^{13}C are presented together with theoretical curves as discussed in the text.

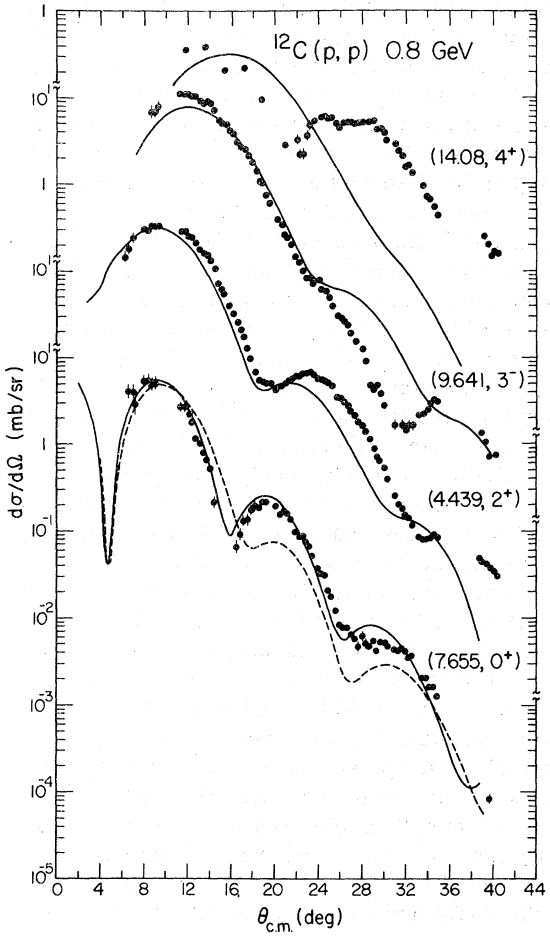

FIG. 6. Angular distribution of transitions to the 4.4, 7.7, 9.6, and 14.1 MeV states in ^{12}C, together with the results of DWBA calculations.

spin-dependence is not well reproduced in the high-momentum transfer region (see Fig. 2 of Ref. 42). Rather, these terms demonstrate the degree of sensitivity which will be afforded by the data, once all first order and important higher order terms are properly treated.

The difference between the RL neutron and the proton rms radii (from electron scattering) for ^{12}C(^{13}C) is 0.07(0.24) fm with an estimated un certainty of ±0.1 fm. Most of this uncertainty results from ambiguities in the spin-dependent amplitudes. The uncertainty in $\langle r^2\rangle_n^{1/2}$ due to spin amplitudes is much smaller for nuclei we have studied other than ^{12,13}C. The actual error in the relative difference between the ^{12}C and ^{13}C neutron radii is probably smaller, since the spin uncertainties should roughly cancel. To make a more quantitative statement would require that analyzing power data be fitted for ^{12}C and ^{13}C, which is not possible at present due to the lack of ^{13}C data.

Both the present analysis of ^{12}C and that of Ahmad[11] are consistent with $\langle r_p^2\rangle^{1/2} = \langle r_n^2\rangle^{1/2}$, but since setting $\rho_n(r) = \rho_p(r)$ gives such a poor result at the back angles, the present analysis implies slightly different *shapes* for proton and neutron matter densities. In comparing the total matter radii for ^{12}C and ^{13}C, defined by

$$\langle r^2\rangle_m^{1/2} = [(Z/A)\langle r_p^2\rangle + (N/A)\langle r_n^2\rangle]^{1/2},$$

one finds indeed that the relative size of ^{13}C to ^{12}C is 1.032 as compared to the ratio of $A^{1/3}$ of 1.027.

The inelastic data and DWBA predictions for $p + ^{12}$C exciting the 2^+, 0^+, 3^-, and 4^+ states are shown in Fig. 6. The excitation of the (2^+, 4.439 MeV) state is well described by the collective model assuming a single step reaction.[59] The deformation length, $|\beta_2 R| = 1.45$ fm is consistent with (10%) the results of several low energy analyses,[59,60] and with that used by Ray[15] to fit 1 GeV data. The deformation of the spin orbit potential, and its contribution to the inelastic form factor, must also be studied for this case.[53]

The (3^-, 9.641 MeV) state in ^{12}C is well reproduced by the DWBA prediction to about 25°(c.m.), with $|\beta_3 R| = 1.02$ fm, which also agrees with (7%) the value used in a previous analysis of 1 GeV inelastic scattering data,[15] and with the average result of several low-energy analyses by Satchler.[59] Note that the observed minimum and maximum in the data near 36° is not predicted by the DWBA calculation. The Saclay 1 GeV data[5] did not reach this region of momentum transfer and thus did not include a minimum. Many calculations have been performed for this inelastic transition in an effort to describe the smoothly falling back angle region of the 1 GeV Saclay data[5] using a variety of nuclear transition density models,[8-11,13,16] but with no better results than that shown in Fig. 6. Analyses which use less realistic models for the density distributions, such as the two or three parameter Fermi model, are unable to avoid predicting very sharp maxima and minima near 25°. As Ray[15] pointed out, the relatively smooth result here is due mainly to the use of the realistic modified charge density of Sick and McCarthy[46] along with a search on the neutron density. A coupled-channels prediction for this state using a deformed-vibrational model[61] gives results that are nearly identical to the DWBA prediction. Even calculations which use empirical inelastic transition densities obtained from electron inelastic scattering do not resolve this discrepancy,[19] but instead also give a result very similar to that seen in Fig. 6.

Both DWBA and coupled channels calculations using a collective model (breathing mode) form factor for the (0^+, 7.655 MeV) state in ^{12}C predict angular distributions which are grossly out-of-phase with the data. Gustafsson and Lambert[19] have shown that form factors based upon particle-hole excitations are able to reproduce both the electron and the 1 GeV proton inelastic scattering data. The transition density used is

$$F_t(r) = V_0 r^t (a + br^2 + cr^4)\exp(-dr^2), \qquad (6)$$

where, for the 0^+ state, $|V_0| = 710$ MeV fm^3, $a = 0.132$ fm^{-3}, $b = -0.023$ fm^{-5}, $c = 0$, and $d = 0.263$ fm^{-2}, assuming a $(1s)^{-1}(2s)$ particle-hole excitation; whereas, one gets $|V_0| = 710$ MeV fm^3, $a = 0.0707$ fm^{-3}, $b = 0.02$ fm^{-5}, $c = -0.00447$ fm^{-7}, and $d = 0.321$ fm^{-2} from an assumed superposition of $(1s)^{-1}(2s)$ and $(1p)^{-1}(2p)$ excitations. These two alternate transition densities were used to obtain the fits shown in Fig. 6. The solid curve results from the two component wave function, while the dashed curve represents the one component prediction. Note that the deep minimum at 16° is better reproduced by the two component model, as was also found in the 1 GeV analysis of Gustafsson and Lambert.[19]

The DWBA prediction for the (4^+, 14.08 MeV) state in ^{12}C, with $|\beta_4 R| = 0.3$ fm, is shown in Fig. 6. Previous 1 GeV Saclay data, as reported in an analysis by Abgrall *et al.*,[13] consist of a few preliminary points, with large statistical errors. There is a factor of three difference in magnitude from that found here. The prediction assuming a spherically symmetric ground state density and a single step mechanism, as shown in Fig. 6, clearly fails to describe the data. A coupled channels calculation, with a deformed potential and inclusion of the 0^+ ground state, 2^+, 4.4 MeV state, 4^+, 14.1 MeV state band via rotational coupling in an exact Legendre polynomial decomposition,[61] has been shown elsewhere to give a very good representation of the inelastic data for the 4^+, 14.1 MeV transition.[48]

We now turn to a discussion of the results of ^{13}C inelastic transitions. The data and DWBA results for five excited states of ^{13}C are shown in Fig. 7.

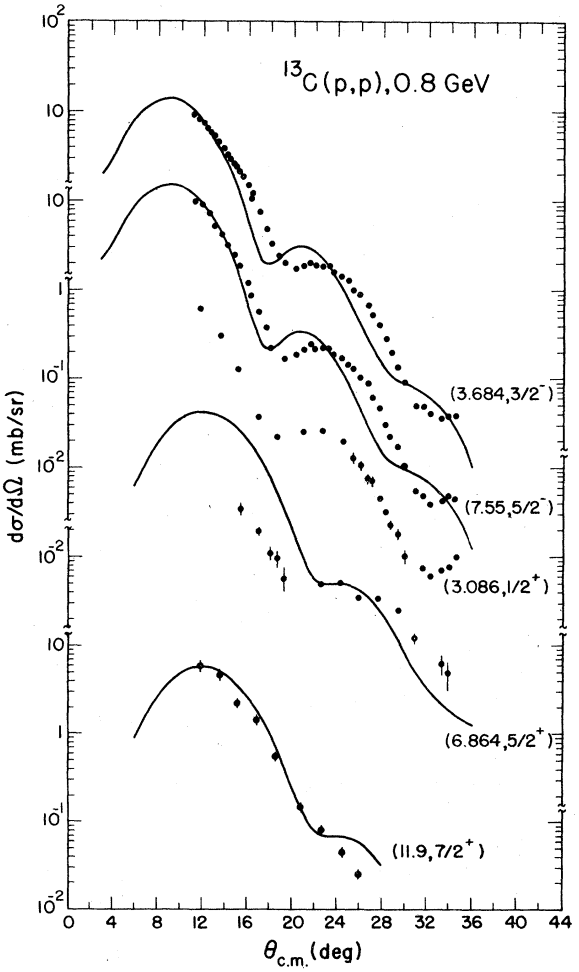

FIG. 7. The angular distributions of protons exciting the 3.1, 3.7, 6.9, 7.6, and 11.9 MeV states in ^{13}C, together with DWBA results.

For targets like ^{13}C that have nonzero ground state spins, the final state angular momentum J_f is ambiguous for a given l transfer. A microscopic calculation should therefore be performed for the transition probabilities, in which one makes use of shell-model nuclear wavefunctions for the ground and excited states, and a two-nucleon effective interaction (or t matrix at these energies), such as the analysis presented by Greaves *et al.*[62] For now, a simpler macroscopic core-excitation model has been adopted, in which it is assumed that the $p_{1/2}$ neutron is weakly coupled to the 2^+ and 3^- excited states of the ^{12}C core. The ($\frac{3}{2}^-$, 3.7 MeV) and the ($\frac{5}{2}^-$, 7.6 MeV) states of ^{13}C are thus assumed to result from the coupling of the $p_{1/2}$ single neutron state to the excited 2^+ core. For a $J=\frac{1}{2}$ ground state, the weak-coupling model and the strong-coupling rotational model predict [63] the same results for the relative strengths of the ^{13}C states compared to the ^{12}C 2^+ core. For the same deformation, the DWBA predicts the ratio of the $\frac{3}{2}^-$ ($\frac{5}{2}^-$) cross section to that of the 2^+ state to be about 0.47 (0.70) at the first maximum, while the experimental value is 0.32 (0.35). The resulting DWBA predictions with $j=l=2$ ($s=0$) are shown in Fig. 7, with a deformation length for the $\frac{3}{2}^-$ ($\frac{5}{2}^-$) state of 1.44 (1.23) fm. The experimental resolution of $\geq$200 keV for protons scattering on ^{13}C does not completely resolve the ($\frac{3}{2}^-$, 3.7 MeV) and the ($\frac{5}{2}^+$, 3.85 MeV)[64] states. As seen in Fig. 3, the 3.85 MeV state appears in the tail of the 3.7 MeV state. Since the 3.7 MeV and the 3.1 MeV states were fit with the same "line shape," the resulting 3.7 MeV cross section should contain very little contribution from the 3.85 MeV state. The ($\frac{5}{2}^-$, 7.547 MeV) state is not resolved from the 7.49 MeV state.[64] Since the line shape of the peak does not differ greatly from other peaks in the spectrum, the contribution of the 7.49 MeV state to the cross section, shown in Fig. 7, is believed to be small.

Ajzenberg-Selove[64] give a tentative spin assignment of $J^\pi=(\frac{7}{2}^-, \frac{5}{2}^+)$ to a state at 11.97 MeV. The state labeled 11.9 MeV in Fig. 3 has been determined to be at an excitation of 11.92 ± 0.06 MeV. In the weak coupling model a $\frac{7}{2}^-$ state would result from a $[p_{1/2}\otimes 4^+]$ configuration. DWBA calculations assuming an $l=4$ transfer fail to reproduce the data. If instead, a $[p_{1/2}\otimes 3^-]$ coupling is assumed, the shape of the predicted cross section using $l=3$ is in agreement with the data. Although the calculations are strongly dependent upon l, they are not particularly j dependent, and thus $J^\pi=\frac{5}{2}^+$ and $\frac{7}{2}^+$ have been used with a resulting $\beta_3 R=1.32$ and 1.14 fm, respectively. The ratio of the 11.9 MeV state's cross section at the first maximum to that for the ^{12}C 3^- state is 0.55 as compared to 0.50 and 0.67 for DWBA predictions (with $J^\pi=\frac{5}{2}^+$ and $\frac{7}{2}^+$) that assume the same deformation. The $J^\pi=\frac{5}{2}^+$ assignment is in agreement with the $\alpha+^9Be$ resonance study (1.93 MeV) of Saleh *et al.*[65] Also, this state could be the same as that seen in 40 MeV ^3He inelastic scattering at an excitation of 11.84 ± 0.03 MeV.[66] The ^3He angular distribution for the state is similar in shape to that for the ^{12}C 3^- state with a ratio of the magnitudes of about 0.3 to 0.4, in general agreement with the above results. Further experimental work is needed to determine fully the spin-parity assignment of this state. Experimental resolution of better than 50 keV is unnecessary since the states in this region have an intrinsic width of $\geq$50 keV.[64]

The $\frac{5}{2}^+$ state at 6.9 MeV is a factor of 10 weaker than the 11.9 MeV state and probably cannot be considered a $[p_{1/2}\otimes 3^-]$ weakly coupled configuration but, perhaps more realistically, a $1d_{5/2}$ single-particle state. An $l=3$ DWBA prediction is shown in Fig. 7 for comparison with the data, using $|\beta_3 R|=0.34$ fm. The ($\frac{1}{2}^+$, 3.1 MeV) state is populated with a strength similar to the ($\frac{5}{2}^+$, 6.9 MeV) state and has been described well in the microscopic analysis of Greaves *et al.*[62] as a $1p_{1/2}$ to $2s_{1/2}$ single-particle transition. For the present, no attempt has been made to repeat such a microscopic calculation at 0.8 GeV. In order for a microscopic calculation to yield good agreement with the ^{13}C data, the theoretical model, that generates the wave functions, must include both the collective quadrupole and octupole contribution of the core. Unfortunately "realistic" calculations usually do not include states above 10 MeV.[67,68]

V. CONCLUSIONS

The purpose of this work was principally to present new data for elastic and inelastic proton scattering from $^{12,13}C$ and ^{208}Pb at 800 MeV. Previous data at 1 GeV incident proton energy provided examples of only a few inelastic transitions. The present work provides enough examples, for ^{12}C and ^{13}C as well as ^{208}Pb, that a number of trends can be identified and a number of preliminary conclusions can be drawn, on the basis of the DWBA analyses.

For the angular distributions of protons scattering on ^{208}Pb, the results of the optical model and DWBA calculations agree rather satisfactorily with the data. (A slight discrepancy seen here in slope between calculation and data for the elastic transition is removed by inclusion of Pauli correlations,[18] while much of the considerably larger discrepancy in slope seen for the inelastic transitions can be removed by inclusion of the spin-orbit terms omitted from the inelastic form factor in the

present calculations.[53]) Most important, the *magnitudes* of the inelastic angular distributions are well described using the same transition strengths as obtained in low-energy studies of the states of ^{208}Pb.

For ^{12}C, one expects and finds that the results of the optical model and DWBA calculations are not very satisfactory. Nonetheless, the fits for the 4.4 MeV 2^+ and 9.6 MeV 3^- angular distributions are found to be as good as or better than those obtained by previous, often more sophisticated, analyses.[9-11,13] The fit to the 7.6 MeV 0^+ transition is consistent with previous results at 1 GeV,[19] while the very poor fit to the 14.1 MeV 4^+ transition indicates the importance of deformation effects and multistep inelastic excitation. We have elsewhere[48] shown that a good fit for this inelastic cross section *is* possible within a coupled-channels approach. It would be expected that Pauli correlations and the deformed spin-orbit term would also play a role for the ^{12}C cross sections, and a full analysis should include these corrections within the coupled channels approach.

Finally, the inelastic cross sections for the states of ^{13}C are rather poorly explored, even at low energies. The present analysis relies heavily on the ^{12}C results, using a model of ^{13}C in which single particle excitations are coupled to ^{12}C core excitations. A fair description is obtained for the 3.7 MeV $\frac{3}{2}^-$ and 7.5 MeV $\frac{5}{2}^-$ transitions, while the model implies that the 11.9 MeV state is populated largely by $l=3$ via the $p_{1/2}$ neutron, coupled to the 3^-, 9.6 MeV state of ^{12}C, and therefore should be assigned $(\frac{5}{2}, \frac{7}{2})^+$. The results indicate a large collective quadrupole and octupole contribution to these states.

In summary, it does not appear that the analysis of medium energy inelastic scattering data presents any insuperable theoretical problems. A somewhat more sophisticated analysis than the present one should readily yield an abundance of new and reliable nuclear structure information, and the success of the present approach should encourage the study at medium energy of a number of other target nuclei in the broad mass region between carbon and lead.

We gratefully acknowledge the support of the accelerator staff at LAMPF during this tune-up experiment of the HRS. The HRS users group, in which several universities are represented, and LASL employees all deserve special credit for their work in evolving an experimental facility that can produce high quality data.

---

†Research supported by the U. S. Department of Energy and The Robert A. Welch Foundation.

‡Present address, New Mexico State University, Las Cruces, New Mexico 88001.

§Present address, Los Alamos Scientific Laboratory, Los Alamos, New Mexico 87545.

¶Present address, Formal Computers Inc., Los Angeles, California 90024.

[1]H. Palevsky *et al.*, Phys. Rev. Lett. 18, 1200 (1967).

[2]G. D. Alkhazov *et al.*, Phys. Lett. 42B, 121 (1972).

[3]G. D. Alkhazov *et al.*, in *High Energy Physics and Nuclear Structure*, edited by G. Tibell (North-Holland, Amsterdam, 1973), p. 176.

[4]J. Thirion, see Ref. 3, p. 168.

[5]R. Bertini *et al.*, Phys. Lett. 45B, 119 (1973).

[6]G. S. Blanpied *et al.*, Phys. Rev. Lett. 39, 1447 (1977).

[7]J. P. Auger and R. J.Lombard, Phys. Lett. 45B, 115 (1973).

[8]I. Brissaud, L. Bimbot, Y. Le Bornec, B. Tatischeff, and N. Willis, Phys. Lett. 48B, 319 (1974).

[9]Y. Alexander and A. S. Rinat, Ann. Phys. (N.Y.) 82, 301 (1974).

[10]R. D. Viollier, Ann. Phys. (N.Y.) 93, 335 (1975).

[11]I. Ahmad, Nucl. Phys. A247, 418 (1975).

[12]E. Kujawski and J. P. Vary, Phys. Rev. C 12, 1271 (1975).

[13]Y. Abgrall, J. Labarsouque, and B. Morand, Nucl. Phys. A271, 477 (1976).

[14]W. R. Coker, L. Ray, and G. W. Hoffmann, Phys. Lett. 64B, 403 (1976).

[15]L. Ray, Ph.D. dissertation, University of Texas, 1977 (unpublished).

[16]G. Alberi, M. Gmitro, and L. Hambro, Nuovo Cimento 38, 239 (1977).

[17]G. K. Varma and L. Zamick, Phys. Rev. C 16, 308 (1977).

[18]E. Boridy and H. Feshbach, Ann. Phys. (N.Y.) 109, 468 (1977); D. R. Harrington and G. K. Varma (unpublished).

[19]C. Gustafsson and E. Lambert, Ann. Phys. (N.Y.) 111, 304 (1978).

[20]H. Rebel (unpublished).

[21]J. W. Negele, Phys. Rev. C 1, 1260 (1970); C 9, 1054 (1974).

[22]D. Vautherin and D. M. Brink, Phys. Rev. C 5, 626 (1972); J. W. Negele and D. Vautherin, 5, 1472 (1972).

[23]J. Saudinos and C. Wilkin, Annu. Rev. Nucl. Sci. 24, 341 (1974); D. M.Corley *et al.*, Nucl. Phys. A184, 437 (1972).

[24]J. P. Auger, J. Gillespie, and R. J. Lombard, Nucl. Phys. A262, 372 (1976).

[25]See AIP document No. PAPS PRVCA 18-1436-38 for 38 pages of numerical data for 0.8 MeV elastic scattering of protons from ^{12}C, ^{13}C, and ^{208}Pb. Order by PAPS number and journal reference from American Institute of Physics, Physics Auxiliary Publications Service, 335 East 45th Street, New York, New York 10017. The prices are $1.50 for microfiche or $6.20 for photocopies. Airmail additional. Make checks payable to the American Institute of Physics. This material also appears in *Current Physics Microfilm*,

the monthly microfilm edition of the complete set of journals published by AIP, on frames immediately following this journal article.
[26]B. Zeidman, Los Alamos Scientific Laboratory Report No. LA-4773/MS, 1971 (unpublished), Pt. I.
[27]H. B. Willard *et al.*, Phys. Rev. C 14, 1545 (1976).
[28]K. Abe *et al.*, Phys. Rev. D 12, 1 (1975).
[29]A. K. Kerman, H. McManus, and R. M. Thaler, Ann. Phys. (N.Y.) 8, 551 (1959).
[30]H. Feshbach, A. Gal, and J. Hüfner, Ann. Phys. (N.Y.) 66, 20 (1971).
[31]J. Lynch and W. R. Coker (unpublished).
[32]E. Boridy and H. Feshbach, Phys. Lett. 50B, 433 (1974).
[33]J. Bystricki, F. Lehar, and Z. Janout, Report No. CEA-N-1547(E)-Saclay-Aout, 1972 (unpublished).
[34]O. Benary, L. R. Price, and G. Alexander, LBL Report No. UCRL-20000NN (unpublished).
[35]T. J. Devlin *et al.*, Phys. Rev. D 8, 136 (1973).
[36]A. A. Vorobyov *et al.*, Phys. Lett. 41B, 639 (1972).
[37]G. Igo, *High Energy Physics and Nuclear Structure*, edited by D. E. Nagle *et al.* (AIP, New York, 1975), p. 70.
[38]W. Grien and P. Kroll (unpublished); A. A. Carter and D. V. Bugg, Phys. Lett. 20, 203 (1964).
[39]R. D. Carlini, dissertation, University of New Mexico, 1977 (unpublished).
[40]M. J. Moravcsik, *The Two-Nucleon Interaction* (Clarendon, Oxford, 1963).
[41]H. Willard, Bull. Am. Phys. Soc. 23, 535 (1978).
[42]G. W. Hoffmann *et al.*, Phys. Rev. Lett. 40, 1256 (1978).
[43]S. I. Bilen'kaya, Yu. M. Kazarinov, and L. I. Lapidus, Zh. Eksp. Teor. Fiz. 60, 460 (1971) [Sov. Phys. JETP 33, 247 (1971)].
[44]C. W. de Jager, H. de Vries, and C. de Vries, At. Data Nucl. Data Tables 14, 479 (1974).
[45]J. Heisenberg, J. S. McCarthy, and I. Sick, Nucl. Phys. A157, 435 (1970).
[46]I. Sick and J. S. McCarthy, Nucl. Phys. A150, 631 (1970).
[47]B. Frois *et al.*, Phys. Rev. Lett. 38, 152 (1977).
[48]L. Ray, G. Blanpied, W. R. Coker, R. Liljestrand, and G. W. Hoffmann, Phys. Rev. Lett. 40, 1547 (1978).
[49]L. Ray, G. W. Hoffmann, G. S. Blanpied, W. R. Coker, and R. P. Liljestrand (unpublished); L. Ray, W. R. Coker, and G. W. Hoffmann (unpublished).
[50]G. R. Satchler, Nucl. Phys. A55, 1 (1964).
[51]R. J. Glauber, in *Lectures in Theoretical Physics*, edited by W. E. Brittin and L. G. Dunham (Interscience, New York, 1959), p. 315.
[52]L. J. Tassie, Aust. J. Phys. 9, 407 (1956).
[53]L. Ray and W. R. Coker (unpublished).
[54]T. Tamura, W. R. Coker, and F. Rybicki, Comp. Phys. Commun. 2, 94 (1971).
[55]G. K. Varma and L. Zamick (unpublished).
[56]W. T. Wagner, G. M. Crawley, G. R. Hammerstein, and H. McManus, Phys. Rev. C 12, 757 (1975).
[57]M. Lewis, F. Bertrand, and C. B. Fulmer, Phys. Rev. C 7, 1966 (1973).
[58]A. Scott, N. P. Mathur, and F. Petrovich, Nucl. Phys. A285, 222 (1977).
[59]G. R. Satchler, Nucl. Phys. A100, 497 (1967).
[60]E. L. Petersen, I. Šlaus, J. W. Verba, R. F. Carlson, and J. R. Richardson, Nucl. Phys. A102, 145 (1967); J. L. Friedes *et al.*, *ibid.* A104, 294 (1967).
[61]T. Tamura, Rev. Mod. Phys. 37, 679 (1965).
[62]P. D. Greaves, V. Hnizdo, J. Lowes, and O. Karban, Nucl. Phys. 179, 1 (1972).
[63]D. Dehnhard and N. M. Hintz, Phys. Rev. C 1, 460 (1970).
[64]F. Ajzenberg-Selove, Nucl. Phys. A268, 1 (1976).
[65]Z. A. Saleh, F. Machali, I. I. Bondouk, and D. A. Darwish, Ann. Phys. (Leipzig) 7, 76 (1974).
[66]G. C. Ball and J. Cerny, Phys. Rev. 177, 1466 (1969).
[67]M. R. Meder and J. E. Purcell, Phys. Rev. C 12, 2056 (1975).
[68]E. C. Halbert, Y. E. Kim, and T. T. S. Kuo, Phys. Lett. 20, 657 (1966).